THERMAL ANALYSIS OF METAL FOAM HEAT SINK SUBJECTED TO IMPINGEMENT JET COOLING

Prof. Karima E. Amori **Deyhaa A. Khalaf**
Mechanical Eng. Dept.
Baghdad University
drkarimaa@yahoo.com

ABSTRACT :
Jet impingement cooling is critical in many industrial applications (such as manufacturing process, gas turbine blades, etc), since it yields high local or averaged heat transfer coefficient, so a large amount of heat is extracted from hot surface. In this work the thermal characteristic of confined impinging air jet on a hot plate is evaluated experimentally and computationally. The parameters studied were , jet Reynolds number (ranged from 14000 to 70000), angle of impingement jet (0^o to 50^o measured from vertical axis on the hot plate), and the heat flux subjected on the hot plate (ranged from 1500 to 6000 W/m^2). The two – dimensional continuity, Navier-Stockes, energy equations with (k-ε) turbulence model have been solved using finite volume method. The effect of covering the hot plate by a layer of Aluminum metal foam have on the impinging jet cooling of this plate is investigated experimentally for the same studied parameters. The experimental and computational results show that increasing the jet angle decreases the Nussetl no. , while increasing Re no. increases Nusselt no. Utilizing a layer of metal foam on the hot plate enhances the heat transfer by jet cooling by 33 % compared with jet cooling of bare hot plate under the same conditions. A comparison of the present results with the available reported data shows good agreement.
Keywords: jet impingement, metal foam, porous heat sink

تحليل حراري لرغوة معدنية تعمل كمصب حراري معرض للتبريد بالنفث التصادمي

أ.د. كريمة اسماعيل عموري **ضياء عبد الرحيم خلف**
قسم الهندسة الميكانيكية/جامعة بغداد

يعتبر التبريد بالنفث التصادمي مهما في التطبيقات الصناعية (كعمليات التصنيع، تبريد ريش التوربين وغيرها) لما يمتلكه من معامل انتقال حرارة عالي لذا يمكن سحب كمية كبيرة من الفيض الحراري من السطوح الساخنة. الهدف من هذا العمل هو تقييم عملي وعددي للمواصفات الحرارية لنفث تصادمي محجوز يضرب صفيحة معدنية ساخنة. المنغيرات التي تم دراستها هي عدد رينولدز بمدى (من 14000 الى 70000)، زاوية النفث الصادم(0 الى 50° مقاسة من المحور العمودي على الصفيحة الساخنة)، وكذلك الفيض الحراري المسلط على الصفيحة الساخنة (امتد من 1500 ال 6000 واط/م^2). حلت معادلة الاستمرارية ، نافير ستوكس ومعادلة الطاقة مع نموذج الاضطراب (k-ε) لحالة ثنائية البعد عدديا باسنخدام طريقة الحجوم المحددة. تم دراسة تأثير تغطية الصفيحة بطبقة من الرغوة المعدنية من مادة الألمنيوم عمليا على التبريد بالنفث التصادمي ولنفس المتغيرات اعلاه. بينت النتائج العملية والنظرية ان زيادة زاوية النفث قللت قيمة (h)، بينما زيادة عدد رينولدز ادى الى زيادة معامل انتقال الحرارة (h). بينت النتائج العملية تحسن واضح (بمقدار 33%) لعدد نسلت عند استخدام طبقة من الرغوة المعدنية على الصفيحة الساخنة عن الحالة بدون استخدام لهذه الطبقة. تم مقارنة النتائج العملية الحالية مع نتائج سابقة واظهرت توافقا جيدا.

NOMENCLATURE

A	Surface area, m^2	s	Distances from the end of heated portion to the end of domain, m
C	Height of metal foam, m	T	Temperature, ^oC
Cp	Specific Heat Capacity, kJ/ kg.K	t	Time, s
C_f	coefficient of friction	V_o	Jet velocity, m / s
d	Jet width, m	V	Volume, m^3
H	Height of Porous Media, m	x, y	Cartesian coordinates, m
h	Heat Transfer Coefficient, W / m^2 ^oC	**Greek symbols**	
I	Current , Amp	ε	turbulent kinetic energy dissipation rate, m^2/s^2
k	Thermal Conductivity, W / m ^oC	μ	Fluid Dynamic viscosity , kg/m.s
K	Permeability, m^2 turbulent kinetic energy, m^2/s^2	ρ	Density, kg / m^3
L	Length of hot plate, m	μ_e	effective dynamic viscosity, (N.s/m^2)
P	Pressure, N / m^2	φ	Porosity
Q	Power , W	σ	Stefan – Boltzmann constant, W/m^2.K^4
q"	Heat Flux W / m^2	μ_t	turbulent viscosity, (N.s/m^2)
SUBSCRIPTS			
h	Hotwall	avg	Average
c	cold wall	eff	Effective
s	Solid or surface	f	Fluid

1. INTRODUCTION

Jet impingement is a cooling technique used for various engineering applications that require cooling such as cooling of gas turbine blades and electronics components, industrial applications metals cooling, glass tempering, drying of textiles products and paper. A metal foam is a cellular structure consisting of a solid metal An ultra-high strength metal matrix composite foam. Various application for Metal foams because it's have properties which make them suitable for any application because Light-weight construction A wide range of metallic foams have become available recently

Bastawros (1998) showed that a high performance cellular aluminum heat sink removed 2-3 times the heat flux removed by a pin-fin array**. Jang, et al. (2003)** investigated experimentally the heat transfer enhancement of a microchannel heat sink subjected to an impinging jet, its thermal resistance is compared with that of a microchannel heat sink with a parallel flow. Under the condition that the pumping power is 0.072W, the thermal resistance of the microchannel heat sink subject to an impinging air jet is experimentally obtained to be 6.1^{o}C/W, which is enhanced by 48.5% compared with that of the microchannel heat sink with a parallel flow. **Crafton (2004)** investigated the flow field associated with a jet impinging onto a surface at an inclined angle using the image-based technologies of temperature and pressure sensitive paints and particle image velocimetry. The results show that the impingement angle of the jet is the dominant parameter in determining the rate of turning/spreading for the jet. **Zhao et al (2004)** studied the dependence of the effective thermal conductivity of metal foam on the temperature of steel alloy; the results showed that the contribution of the heat transfer by natural convection was also significant. The effective thermal conductivity increased as the

pore size or relative density increased. **Kim (2005)** showed that an aluminium foam heat sink with low pore density is more efficient (by 28%) than a conventional parallel-plate heat sink of the same size. **Salas and Waas (2007)** found that when increasing foam thickness from (6.4mm to 25.4mm)the heat transfer level isincreased, as revealed by a larger convective coefficient and a larger temperature difference between both foam surfaces. **Bentarzi, et al (2011)** presented a computational study of the impingement of two turbulent jets on a solid heated plate, using k-ε model. **Kumar and Prasad (2011)** investigated both computationally and experimentally of conjugate heat transfer from a flat circular disk with a constant heat flux imposed on its bottom surface and a shower head of air jets impinging on the top surface. The shower head consists of a central jet surrounded by four neighboring perimeter jets. **Wong (2012)** conducted an experimental and numerical thermal analysis of metal foam (FeCrAlY) subjected to jet impingement cooling in a horizontal channel.The results show that, the deterioration of heat transfer rate is more significant at higher values of Rayleigh number. **Chen, et al (2012)** conducted a numerical investigation for enhanced heat transfer from multiple discrete heated sources in a horizontal channel by metal-foam porous layer. **Augusto, et al (2012)** evaluated experimentally the spray cooling on a horizontal upward facing 25 mm diameter heater onto which a 5-mm copper foam disk thickness of same diameter was brazed. **Agrawal, et al (2013)** Studied experimentally rewetting behavior of a hot horizontal stainless steel surface during the mist jet impingement cooling.

The objective of this work is to investigate experimentally and computationally the heat transfer between vertical or inclined round confined jet and a horizontal hot surface for a range of impingement parameters .The important target of this work is to reveal the effect of covering the hot surface by a layer of metal foam on the impingement jet cooling of this surface.

2. EXPERIMENTAL SETUP

Fig. (1) shows a schematic diagram and a plate of the experimental setup used in this work. The parameters of this construction are: jet width (2d) is 10 mm, the jet velocity V_o, the temperature difference ($T_h - T_c$) in which T_c is the fluid temperature at the jet inlet whereas T_h is the temperature of the hot plate, the heat source length 2L (where L is the length of hot plate) and the distance from the jet inlet to the heat source h..

The hot plate was made from aluminum of dimensions (100×100×20 mm). It is formed of two-pieces, upper and lower halves. The thermal properties of this metal are given in Table (1). The upper and lower parts of this plate have been drilled (simi-cylindrical shape) to insert four resistive type cartridge heaters of 10 mm in diameter and 100mm in length within it. The upper part has five bores to insert the thermocouples (of type K) to measure the hot plate surface temperature. These heater work as a heat source provide 300 W at full load. Tests are conducted for different air mass flow rates (10, 20, 30, 40 and 50 lpm) and for five constant heats fluxes (15, 22.5, 33, 45.5 and 60 Watt).

A digital thermometer type LUTRON, was used to record 12 temperature readings (five for plate surface temperature, three for heater temperature, air temperature at jet inlet, and two for air at duct exit section, and ambient temperature). The thermometer resolution is 0.1 ^oC, accuracy of $\pm$ 0.4 ^oC % and range of (-100^oC to 1300 ^oC).

The power generated in the present work by heater was measured by a digital (Watt meter type LUTRON DW-6060) of percentage error of (-0.1 %). An air flow meter (float type) was installed to measure the air volume flow rate supplied to the jet nozzle. The range of this flow meter is (0 to 100) lpm

3. ERROR ANALYSIS :-

The accuracy of obtaining experimental results depends upon two factors, the accuracy of measurements and the design details of test rig and human being error. Based on the error analysis approach presented in **Holman (1989)**, the experimental percentage error for Nusselt no. can be calculated as

$$R = R(v_1, v_2, \cdots\cdots, v_n) \tag{1}$$

For small variations in the variables, this relation can be expressed in linear form as

$$\delta R = \frac{\partial R}{\partial v_1}\delta v_1 + \frac{\partial R}{\partial v_2}\delta v_2 + \cdots\cdots + \frac{\partial R}{\partial v_n}\delta v_n \tag{2}$$

……..

Hence, the uncertainty intervals (w) in the result can be given as

$$w_R = \left[\left(\frac{\partial R}{\partial v_1}\cdot w_1\right)^2 + \left(\frac{\partial R}{\partial v_2}\cdot w_2\right)^2 + \cdots\cdots + \left(\frac{\partial R}{\partial v_n}\cdot w_n\right)^2\right]^{0.5} \tag{3}$$

Eq. (3) is greatly simplified upon dividing by Eq. (1) to nondimensionaliz.

$$\frac{w_R}{R} = \left[\left(\frac{\partial R}{\partial v_1}\cdot\frac{w_1}{R}\right)^2 + \left(\frac{\partial R}{\partial v_2}\cdot\frac{w_2}{R}\right)^2 + \cdots\cdots + \left(\frac{\partial R}{\partial v_n}\cdot\frac{w_n}{R}\right)^2\right]^{0.5} \tag{4}$$

The local Nusselt no. is calculated as

$$Nu_x = \frac{(Q_{total} - Q_{conduction} - Q_{radiation})\cdot x}{A_s\cdot(T_w - T_{\infty,x})\cdot k_{eff}} \tag{5}$$

where $Q_{radiation}$ is heat loss from the hot plate which is neglected in this work.

$$Nu_x = \frac{(Q_{total} - Q_{conduction})\cdot x}{A_s\cdot(T_w - T_{\infty,x})\cdot k_{eff}} \tag{6}$$

where

$Q_{total} = I.V_o$ (6a)

$Q_{conduction} = k_{ins}\cdot\frac{\Delta T_{Al}}{\Delta\eta}\cdot A_s$ (6b)

$$Nu_x = \frac{I\cdot V_o\cdot x}{A_s\cdot\Delta T_{w,x}\cdot k_{eff}} - \frac{k_{ins}\cdot\frac{\Delta T_{Al}}{\Delta\eta}\cdot x}{\Delta T_{w,x}\cdot k_{eff}} \tag{7}$$

Based on Eq.6 the Nusselt number is a function of several variables, each subjected to an uncertainty

$$Nu_x = f(V_o, I, x, A_s, \Delta T_{Al}, \Delta T_{w,x})$$

where;

$\Delta T_{Al} = T_{in} - T_{out}$

$\Delta T_{w,x} = T_w - T_{\infty,x}$

$$\frac{\partial Nu_x}{\partial V_o} = \frac{I \cdot x}{A_s \cdot \Delta T_{w,x} \cdot k_{eff}} \quad (8)$$

$$\frac{\partial Nu_x}{\partial I} = \frac{V_o \cdot x}{A_s \cdot \Delta T_{w,x} \cdot k_{eff}} \quad (9)$$

$$\frac{\partial Nu_x}{\partial x} = \frac{I \cdot Vo}{A_s \cdot \Delta T_{w,x} \cdot k_{eff}} - \frac{k_{ins} \cdot \frac{\Delta T_{Al}}{\Delta \eta}}{\Delta T_{w,x} \cdot k_{eff}} \quad (10)$$

$$\frac{\partial Nu_x}{\partial A_{surface}} = -\frac{I\, V_o x}{(A_{surface})^2 \Delta T_{w,x} \cdot k_{eff}} \quad (11)$$

$$\frac{\partial Nu_x}{\partial \Delta T_{Al}} = -\frac{k_{insulator} \cdot \frac{x}{\Delta \eta}}{\Delta T_{w,x} \cdot k_{eff}} \quad (12)$$

$$\frac{\partial Nu_x}{\partial \Delta T_{w,x}} = -\frac{I \cdot Vo \cdot x}{A_s \cdot k_{eff} \cdot \Delta T_{w,x}^2} + \frac{k_{ins} \cdot \frac{\Delta T_{Al}}{\Delta \eta} \cdot x}{k_{eff} \cdot \Delta T_{w,x}^2} \quad (13)$$

Therefore the uncertainty intervals (w) for Nusselt no. can be given as follows;

$$W_{Nu_x} = \left[\left(\frac{\partial Nu_x}{\partial Vo} \cdot W_{Vo} \right)^2 + \left(\frac{\partial Nu_x}{\partial I} \cdot W_I \right)^2 + \left(\frac{\partial Nu_x}{\partial x} \cdot W_x \right)^2 + \left(\frac{\partial Nu_x}{\partial A_s} \cdot W_{A_s} \right)^2 + \left(\frac{\partial Nu_x}{\partial \Delta T_{w,x}} \cdot W_{\Delta T_{w,x}} \right)^2 + \left(\frac{\partial Nu_x}{\partial \Delta T_{Al}} \cdot W_{\Delta T_{Al}} \right)^2 \right]^{0.5} \quad (14)$$

4. THEORETICAL AND NUMERICAL MODEL

The metal foam is assumed to be homogeneous and isotropic. In the present work, the solid matrix of the porous medium is assumed to be in local thermal equilibrium with the fluid and steady state two dimensional incompressible fluid flows. Two sets of governing equations are required to solve the physical problem with fluid=porous interface; one for the porous region, another for the clear fluid region for turbulent flow , these sets are :

4.1 Governing Equations in the fluid region (region I)

1-Continuity Equation:

$$\frac{\partial u}{\partial x} + \frac{\partial v}{\partial y} = 0 \quad (15)$$

2-Momentum Equation :

$$\rho_f \left(u \frac{\partial u}{\partial x} + v \frac{\partial u}{\partial y} \right) = -\frac{\partial p}{\partial x} + \frac{\partial}{\partial x}\left(\mu_f \frac{\partial u}{\partial x} \right) + \frac{\partial}{\partial y}\left(\mu_f \frac{\partial u}{\partial y} \right) \quad (16)$$

$$\rho_f \left(u \frac{\partial v}{\partial x} + v \frac{\partial v}{\partial y} \right) = -\frac{\partial p}{\partial y} + \frac{\partial}{\partial x}\left(\mu_f \frac{\partial v}{\partial x} \right) + \frac{\partial}{\partial y}\left(\mu_f \frac{\partial v}{\partial y} \right) \quad (17)$$

3- Energy Equation:

$$\rho_f cp_f \left(u \frac{\partial T_f}{\partial x} + v \frac{\partial T_f}{\partial y} \right) = \frac{\partial}{\partial x}\left(k_f \frac{\partial T_f}{\partial x} \right) + \frac{\partial}{\partial y}\left(k_f \frac{\partial T_f}{\partial y} \right) \quad (18)$$

4-Turbulence Model:

The turbulence kinetic energy (K) and it's rate of dissipation (ε) are obtained from the following transport equations.Forsteady state two dimensional incompressible fluid flows. Forced convection. Steady and horizontal flow.

$$\frac{\partial}{\partial x}\left[\left(\frac{\mu_e}{\sigma_K}\right)\frac{\partial K}{\partial x}\right]+\frac{\partial}{\partial y}\left[\left(\frac{\mu_e}{\sigma_K}\right)\frac{\partial K}{\partial y}\right]+G_K-\rho\varepsilon=0 \qquad (19)$$

And

$$\frac{\partial}{\partial x}\left[\left(\frac{\mu_e}{\sigma_\varepsilon}\right)\frac{\partial \varepsilon}{\partial x}\right]+\frac{\partial}{\partial y}\left[\left(\frac{\mu_e}{\sigma_\varepsilon}\right)\frac{\partial \varepsilon}{\partial y}\right]+C_{1\varepsilon}G_K\frac{\varepsilon}{K}-C_{2\varepsilon}\rho\frac{\varepsilon^2}{K}=0 \qquad (20)$$

where:

u, v = component of the velocity vector in the x, and y direction.

ρ: Fluid density, kgm^{-3}

Cp: specific heat at constant pressure, $Jkg^{-1}K^{-1}$

For the turbulent case the effective dynamic viscosity (μ_e) is defined as:

$\mu_e = \mu + \mu_t$

where

μ: Laminar dynamic viscosity (fluid property)

μ_t: turbulent viscosity is turbulent model (k-ε) is used to evaluate the turbulent viscosity through the expression is:

$$\mu_t=\rho C_\mu\frac{k^2}{\varepsilon}$$

where:

k: turbulent kinetic energy

ε: turbulent kinetic energy dissipation rate.

In these equations,G_K represents the generation of turbulence kinetic energy due to the mean velocity gradients. C_1andC_2 are constants. $\sigma_k$andσ_ε are the turbulent Prandtl numbers for K and ε, respectively.

The values of turbulence model constants$C_{1\varepsilon}$,$C_{2\varepsilon}$,C_μ , σ_K, and σ_ε are given in Table (3).

The Dimensionless parameters can be used to reduce some parameters are adopted in the present study can be written as:

$$X=\frac{x}{L},Y=\frac{y}{L},S=\frac{s}{L},U=\frac{u}{Vo},V=\frac{v}{Vo},\theta=\frac{T-T_c}{T-T_h} \qquad (21)$$

Equations (15) to (20) are transformed into dimensionless form based on the dimensionless parameters presented in eq. (21), such as:

1-Continuity Equation:

$$\frac{\partial U}{\partial X}+\frac{\partial V}{\partial Y}=0 \qquad (22)$$

2-Momentum Equation :

$$U\frac{\partial U}{\partial X}+V\frac{\partial U}{\partial Y}=-\frac{\partial P}{\partial X}+\frac{Pr}{Pe}\left(\frac{\partial^2 U}{\partial X^2}+\frac{\partial^2 U}{\partial Y^2}\right) \qquad (23)$$

$$U\frac{\partial V}{\partial X}+V\frac{\partial V}{\partial Y}=-\frac{\partial P}{\partial Y}+\frac{Pr}{Pe}\left(\frac{\partial^2 V}{\partial X^2}+\frac{\partial^2 V}{\partial Y^2}\right) \qquad (24)$$

2- Energy Equation:

$$U\frac{\partial\theta}{\partial X}+V\frac{\partial\theta}{\partial Y}=\frac{1}{Pe}\left(\frac{\partial^2\theta}{\partial X^2}+\frac{\partial^2\theta}{\partial Y^2}\right)+\mu\emptyset_v \qquad (25)$$

where

pe is Peclet number and it is calculated as: $Pe=\frac{V_0 L}{\alpha_f}$,

Pr is Prandtl number and it is calculated as: $Pr=\frac{v}{\alpha_f}$,

4 -Turbulence Model:

$$\frac{\partial}{\partial X}\left[\left(\frac{\mu_e}{\sigma_K}\right)\frac{\partial K}{\partial X}\right]+\frac{\partial}{\partial Y}\left[\left(\frac{\mu_e}{\sigma_K}\right)\frac{\partial K}{\partial Y}\right]+L^2(G_K-\rho\varepsilon)=0 \qquad (26)$$

And

$$\frac{\partial}{\partial x}\left[\left(\frac{\mu_e}{\sigma_\varepsilon}\right)\frac{\partial \varepsilon}{\partial x}\right]+\frac{\partial}{\partial y}\left[\left(\frac{\mu_e}{\sigma_\varepsilon}\right)\frac{\partial \varepsilon}{\partial y}\right]+L^2\left(C_{1\varepsilon}G_K\frac{\varepsilon}{K}-C_{2\varepsilon}\rho\frac{\varepsilon^2}{K}\right)=0 \qquad (27)$$

4.2 Governing Equations in The metal foam (region II)

The conservation equations for the two-dimensional steady flow in porous medium for continuity, momentum, and energy are**:**

1-Continuity Equation:

$$\frac{\partial u}{\partial x}+\frac{\partial v}{\partial y}=0 \qquad (28)$$

2-Momentum Equation :

$$\frac{1}{\varphi^2}\left(\rho u\frac{\partial u}{\partial x}+\rho v\frac{\partial u}{\partial y}\right)=-\frac{\partial p}{\partial x}+\frac{\mu}{\varphi}\left(\frac{\partial^2 u}{\partial x^2}+\frac{\partial^2 u}{\partial y^2}\right)-\frac{\mu}{K}u-\frac{C_f\rho}{\sqrt[3]{K}}|v|u \qquad (29)$$

$$\frac{1}{\varphi^2}\left(\rho u\frac{\partial v}{\partial x}+\rho v\frac{\partial v}{\partial y}\right)=-\frac{dp}{dx}+\frac{\mu}{\varphi}\left(\frac{\partial^2 v}{\partial x^2}+\frac{\partial^2 v}{\partial y^2}\right)-\frac{\mu}{K}v-\frac{C_f\rho}{\sqrt[3]{K}}|v|v \qquad (30)$$

3- Energy Equation in Porous Media:

$$u\frac{\partial T}{\partial x}+v\frac{\partial T}{\partial y}=\frac{k_{eff}}{\rho Cp}\left(\frac{\partial^2 T}{\partial x^2}+\frac{\partial^2 T}{\partial y^2}\right) \qquad (31)$$

where

φ: Porosity

C_f: coefficient of friction

K: permeability of the porous medium, m^2

Based on dimensionless terms defined in Eq. (21) the governing equations are transformed into dimensionless forms such as

1-Continuity Equation:

$$\frac{\partial U}{\partial X}+\frac{\partial V}{\partial Y}=0 \qquad (32)$$

2-Momentum Equation :

$$U\frac{\partial U}{\partial X}+V\frac{\partial U}{\partial Y}=-\varphi^2\frac{dP}{dX}+\frac{\varphi Pr}{Pe}\left(\frac{\partial^2 U}{\partial X^2}+\frac{\partial^2 U}{\partial Y^2}\right)-\frac{\varphi^2 Pr}{PeDa}U-\frac{\varphi^2 C_F}{\sqrt[3]{Da}}U\sqrt{U^2+V^2} \qquad (33)$$

$$U\frac{\partial V}{\partial X}+V\frac{\partial V}{\partial Y}=-\varphi^2\frac{dP}{dY}+\frac{\varphi Pr}{Pe}\left(\frac{\partial^2 V}{\partial X^2}+\frac{\partial^2 V}{\partial Y^2}\right)-\frac{\varphi^2 Pr}{PeDa}V-\frac{\varphi^2 C_F}{\sqrt[3]{Da}}V\sqrt{U^2+V^2} \qquad (34)$$

3- Energy Equation in Porous Media:

$$U\frac{\partial \theta}{\partial X}+V\frac{\partial \theta}{\partial Y}=\frac{k_{eff}}{\rho Cp}\left(\frac{\partial^2 \theta}{\partial X^2}+\frac{\partial^2 \theta}{\partial Y^2}\right) \qquad (35)$$

where the

Da is Darcy number, it is defined as

$$Da=\frac{K}{L^2},$$

R_k is Thermal conductivity, it is defined as

$$R_k=\frac{k_{eff}}{k_f}$$

4.2 Boundary conditions

The flow and heat transfer characteristics are symmetrical around the Y-axis, as shown in Figure (2). Due to this symmetry, only one half is considered for the computational purpose and the boundary conditions are:

1- At X=0 (symmetrical axis)

$$\frac{\partial \theta(0,Y)}{\partial X}=U(0,Y)=\frac{\partial V(0,Y)}{\partial X}=0 \qquad (36)$$

2- At X= 1+S (flow exit)

$$\frac{\partial \theta(1+S,Y)}{\partial X}=\frac{\partial U(1+S,Y)}{\partial X}=\frac{\partial V(1+S,Y)}{\partial X}=0 \qquad (37)$$

P=0 (atmospheric pressure)

3- At Y=0 (hot plate and duct surface)

$$U(X,0)=V(X,0)=0 \qquad (38)$$

$$\theta(X,0)=1 \text{ for } 0\leq X\leq 1 \text{ and otherwise}$$

$$\frac{\partial \theta(X,0)}{\partial Y}=0 \qquad (39)$$

4- At Y = 1 (upper surface)

$$U(X,1)=\theta(X,1)=0 \qquad (40)$$

5. NUMERICAL SOLUTION

Fluent program has been used to computationally analyze the confined air jet cooling of hot plate. The first step of simulation is dividing the computational domain into small cells using Gambit program. Differential equations of momentum, energy, and mass balance are solved iteratively until the solution reaches the desired accuracy. A fine mesh is adopted to accurately capture the appropriate details of the fluid flow and heat transfer. Inlet and outlet zones are then meshed using the same manner, with the heating elements surface serving as the source for mesh generation. From many practical tests, a spacing of elements of (0.001 mm) was enough to capture the appropriate variables of fluid flow and heat transfer with convergence criteria of 10^{-5}.

6. RESULTS AND DISCUSSION

The numerical and experimental results of cooling jet flows over a hot plate covered or not covered with a metal foam layer is a presented and analyzed in this work. The effect of jet air velocity on plate, air and heater temperature distribution, as well as on local and average Nusselt number (Nu) is presented.

Figures (3) to (7) depict the variation of local Nusselt number on hot plate surface subjected to 1500 W/m^2 for case I and case II for different Reynolds number and jet angles. Higher local Nusselt number of hot plate covered with metal foam is indicated compared to hot plate not covered with metal foam

Figure (8) shows that the average Nusselt number increases with increasing Reynolds number at constant heat flux. Higher values of average Nusselt number was reported to normal jet compared with oblique one.

Figure (9) shows a decrease in the average Nusselt number for hot plate surface covered or not covered with metal foam with increasing jet tilt angle. A considerable decrease is reported for higher Reynolds number, Also this behavior is obviously shown for plate covered with a layer of metal foam.

Figure(10) presents a considerable variation of average Nu number as Reynolds number increases. This variation be more obvious as the heat flux subjected on the hot plate is decreases. Good agreement is obtained as shown in Fig. (11) when a comparison of local Nusselt number along hot plate surface of the present experimental work was made with the results achieved by **Colucci (1996)** for the same Reynolds number.

A Comparison of the obtained experimental and numerical results for the temperature distribution along hot plate surface is conducted for different Reynolds number and jet tilt angles as illustrated in Fig.(12). The maximum and minimum percentage deviation for average temperature of plate surface are 12.1% 3.6% respectively as given in table (4).

Constant heat flux boundary conditions have been applied. The temperature distributions within the physical domain of confined impinging jet on a heated flat plate are presented in figures (13 to 15) for various air jet velocities. The outlet air temperature increases with the increase of heat flux but decreases with increasing of Reynolds number.

7. CONCLUSIONS

The present work investigates the heat transfer from hot plate surface subjected to impinging jet. According to the previous discussion of the obtained results the following points can be concluded:

Increasing jet Reynolds number increases the heat transfer from the hot plate for all angles of impinging jet. The heat transfer from hot plate increases by using metal foam for any Reynolds number. The heat transfer decreases with increase tilt angle of jet.

Table (1): Thermal properties of aluminum, **Holman (1989)**

Metal	ρ (kg/m^3)	C_P(KJ/kg ^{o}C)	K (W/m ^{o}C)	α (m^2/s)
Aluminum	2700	0.896	220	8.418 ×10-5

Table (2): Uncertainties of Measuring Devices.

Parameter	Temperature	Heater Power	Hydraulic Diameter
Accuracy	± 0.04 ^{o}C	± 0.01 W	± 0.024 m

Table (3) Values of Model Constant are used in K-ε Model

Constant	$C_{1\varepsilon}$	$C_{2\varepsilon}$	C_μ	σ_K	σ_ε
Value	1.44	1.92	0.09	1	1.3

Table (4): Percentage deviation of experimental and computational results of average temperature of hot plate not covered with a metal foam layer for heat flux (1500 W/m^2)

Re No.	Tilt angle α					
	0	10	20	30	40	50
14000	**12.1 %**	6 %	**3.6 %**	10 %	8.9 %	3.69 %
28000	10.8	10.6	10.1	3.7	9.6	8
42000	12	9.3	8.4	11.9	8.75	9.2
56000	14	7	9.1	8	8.3	11.2
70000	8	9	11	7.6	11	9.8

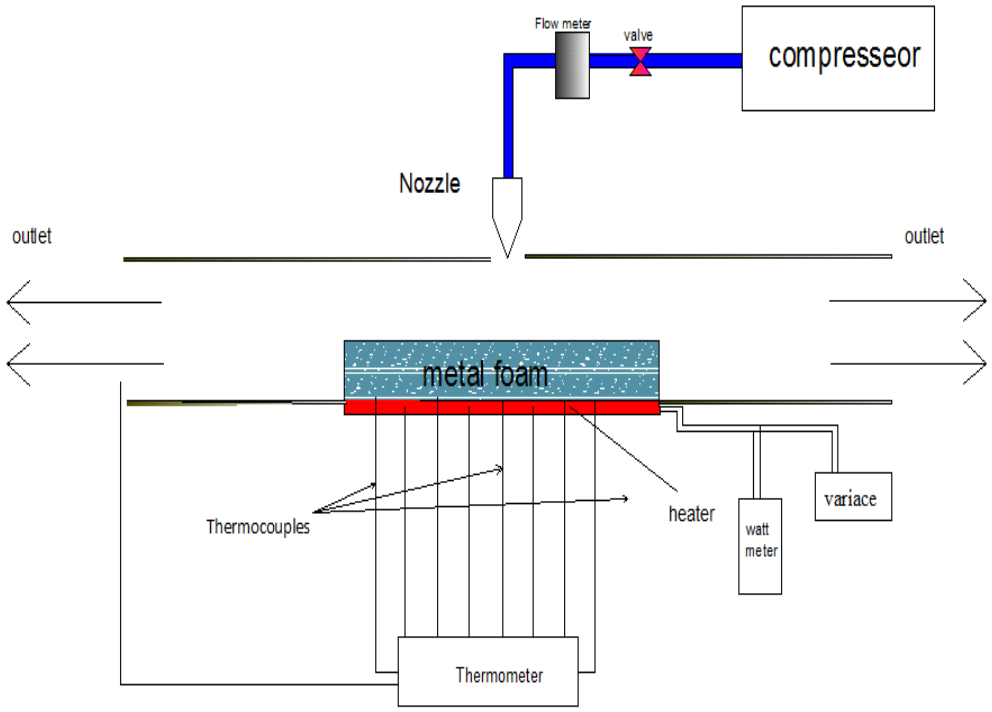

(a)

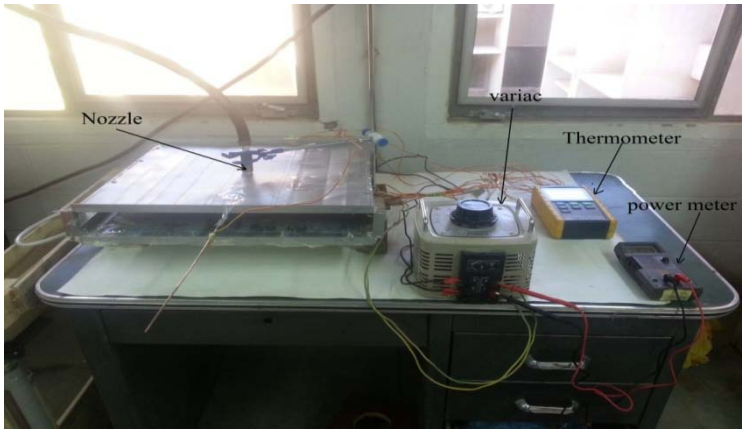

(b)

Fig.(1): a) Schematic diagram of the experimental setup, b) Cartridge heaters and thermocouples inserted within the target plate

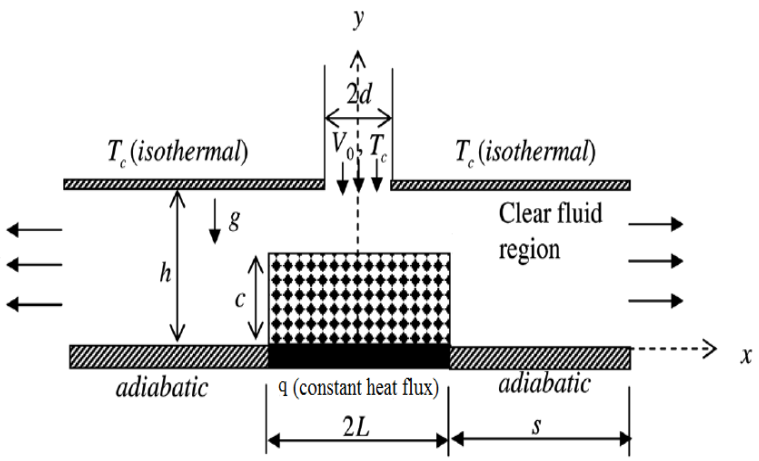

Fig. (2) : Physical model adopted in the numerical study

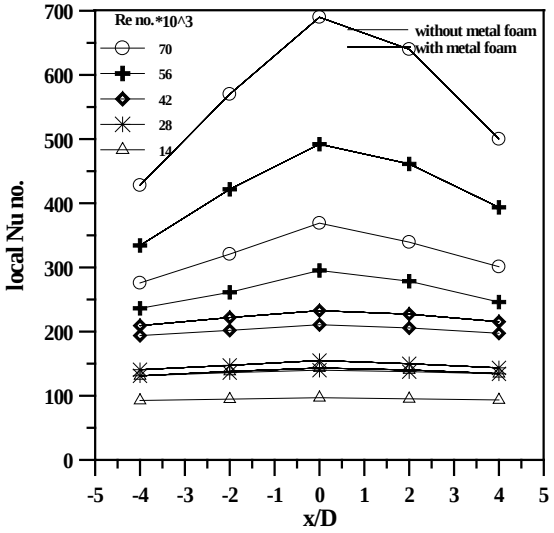

Fig.(3): Distribution of local Nusselt no. along the hot plate covered with and not covered with a layer of metal foam, ($\alpha=0^o$) (exp.)

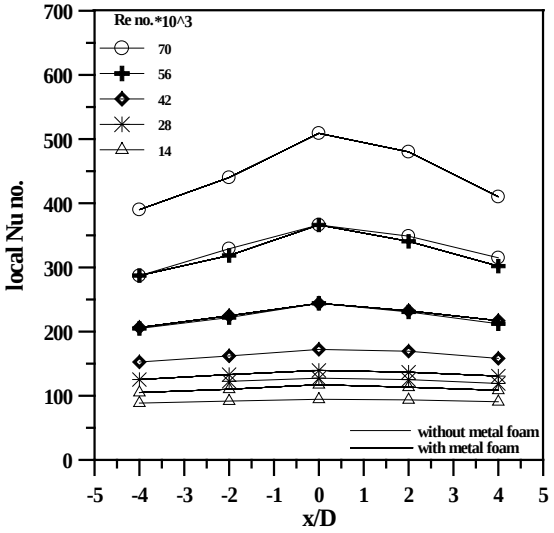

Fig.(4): Distribution of local Nusselt no. along the hot plate covered with and not covered with a layer of metal foam, ($\alpha=10^o$) (exp.)

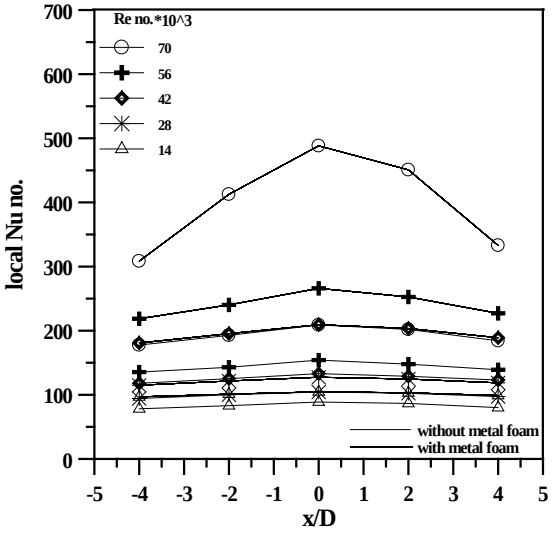

Fig.(5): Distribution of local Nusselt no. along the hot plate covered with and not covered with a layer of metal foam, ($\alpha=20^o$) (exp.)

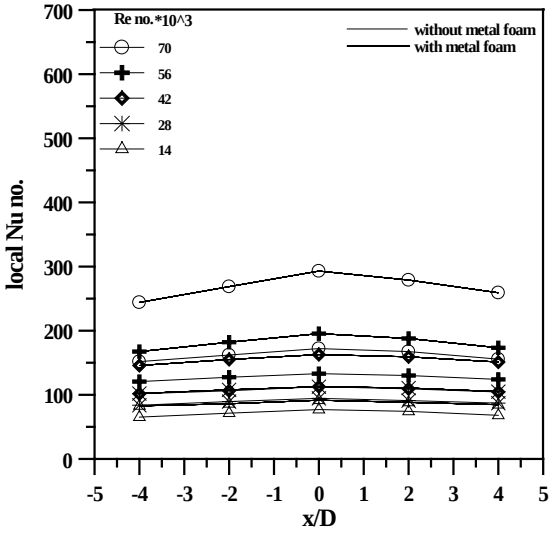

Fig.(6): Distribution of local Nusselt no. along the hot plate covered with and not covered with a layer of metal foam, ($\alpha=30^o$) (exp.)

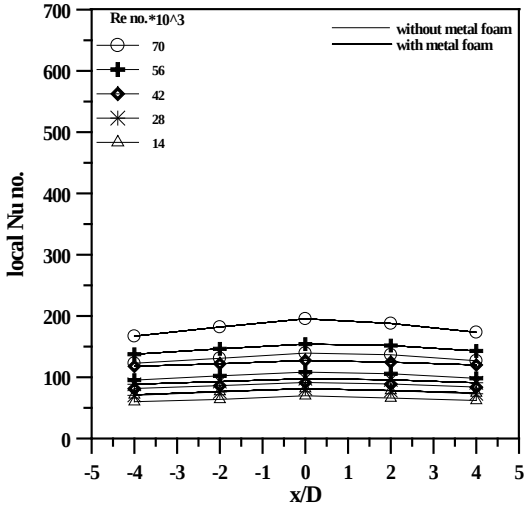

Fig.(7): Distribution of local Nusselt no. along the hot plate covered with and not covered with a layer of metal foam, ($\alpha=40^o$) (exp.)

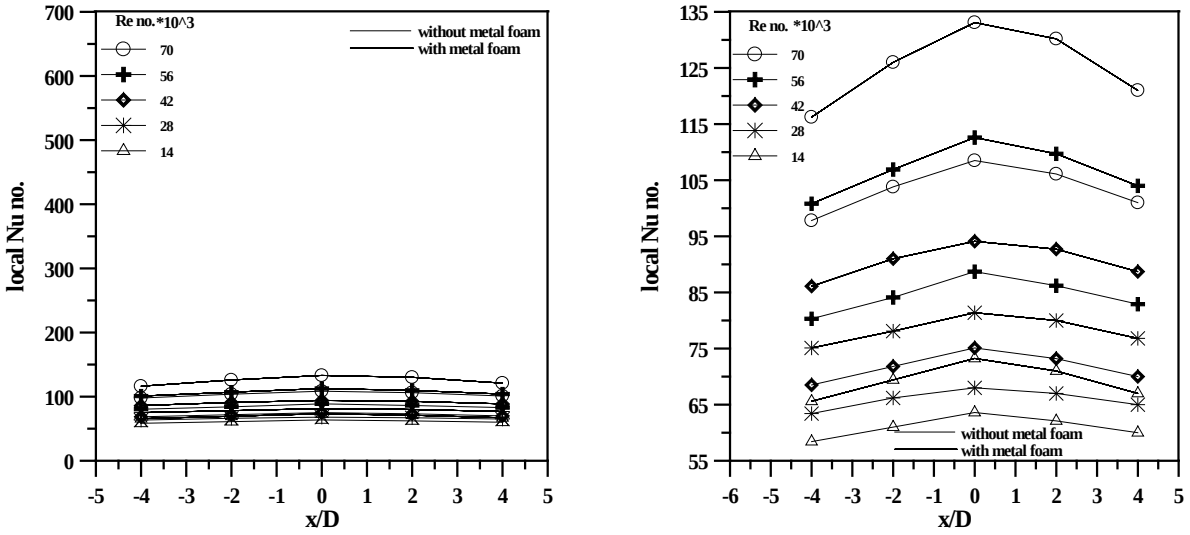

Fig.(8): Distribution of local Nusselt no. along the hot plate covered with and not covered with a layer of metal foam, ($\alpha=50^o$,$q=1500W/m^2$) (exp.) a) full scale, b) enlarged y axis

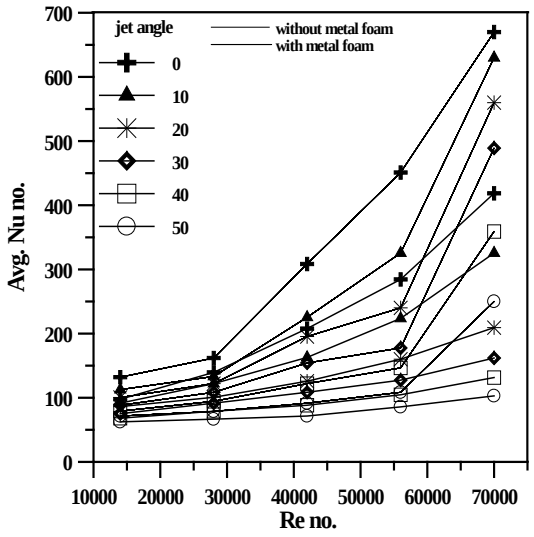

Fig.(9): Variation of average Nusselt no. with Reynolds no. for different jet tilt angles for hot plate covered with and not covered with a layer of metal foam. ($q=1500W/m^2$) (exp.)

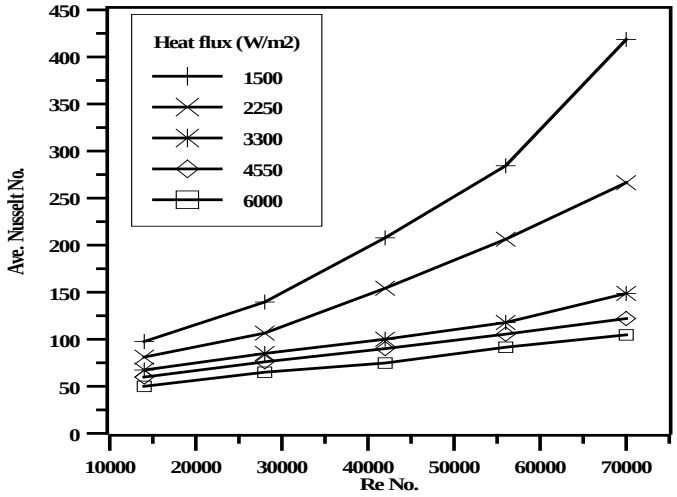

Fig. (10): Variation of Average Nusselt number with Re no. for hot plate not covered with metal foam

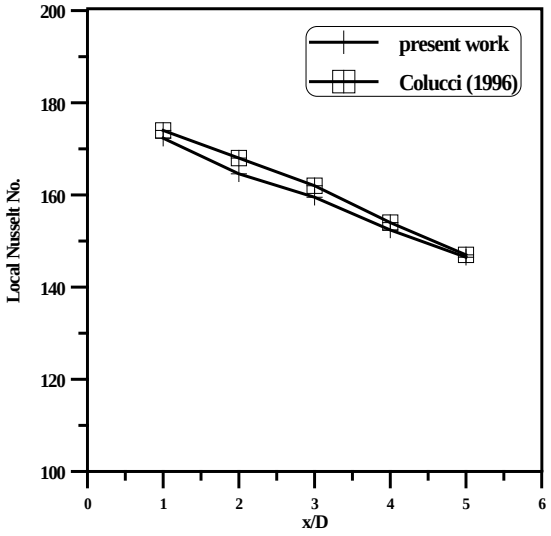

Fig. (11): Local Nusselt Number along the hot plate not covered with metal foam for (q=1500 w/m) for Reynolds number (28000)

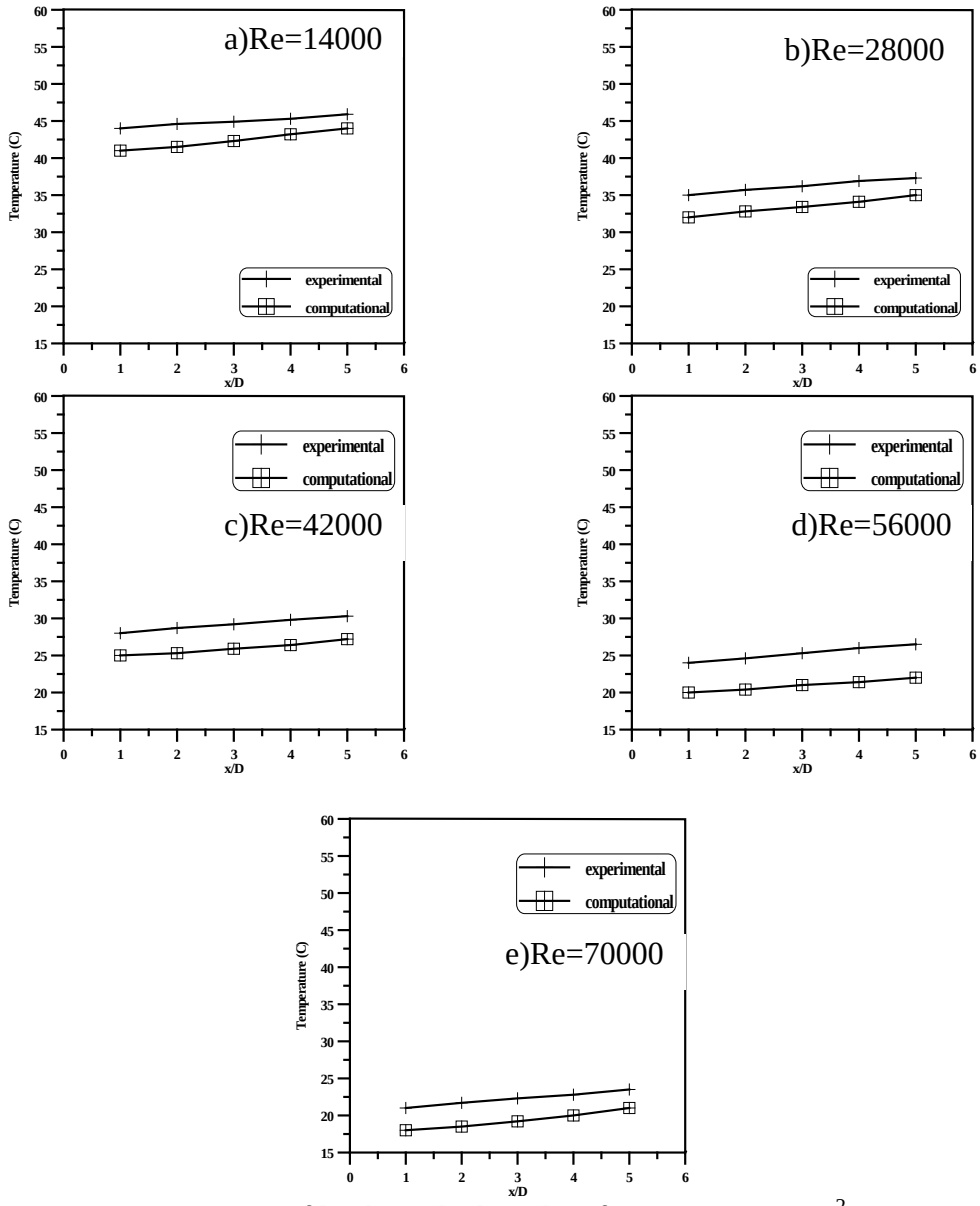

Fig.(12): Temperature Profile along the hot plate for (q"=1500 W/m^2) numerically and experimentally different Reynolds number (α= 0^o)

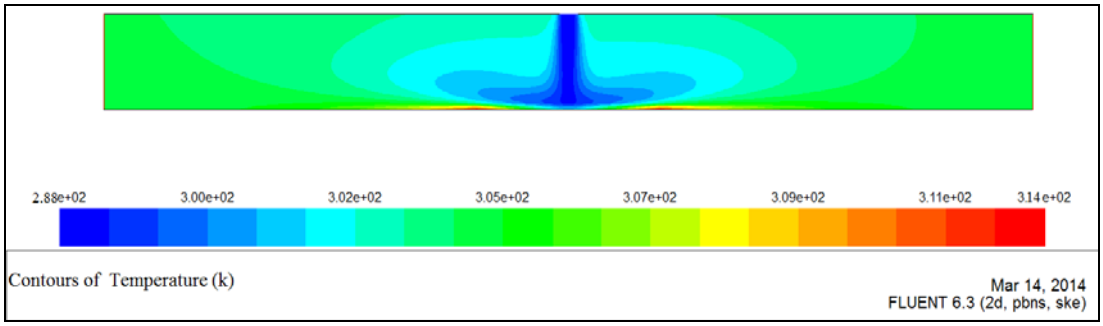

a): (Re=14000)

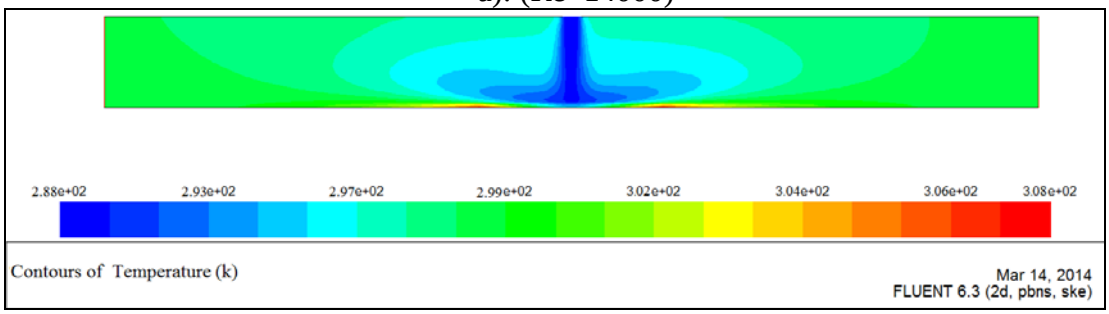

b): (Re=28000)

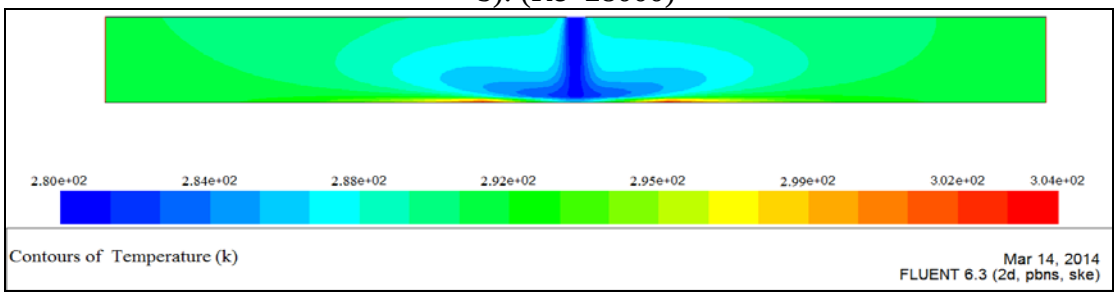

c): (Re=42000)

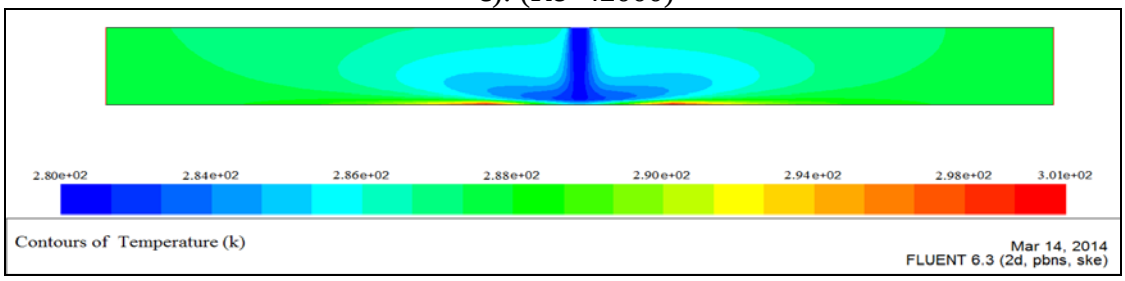

d): (Re=56000)

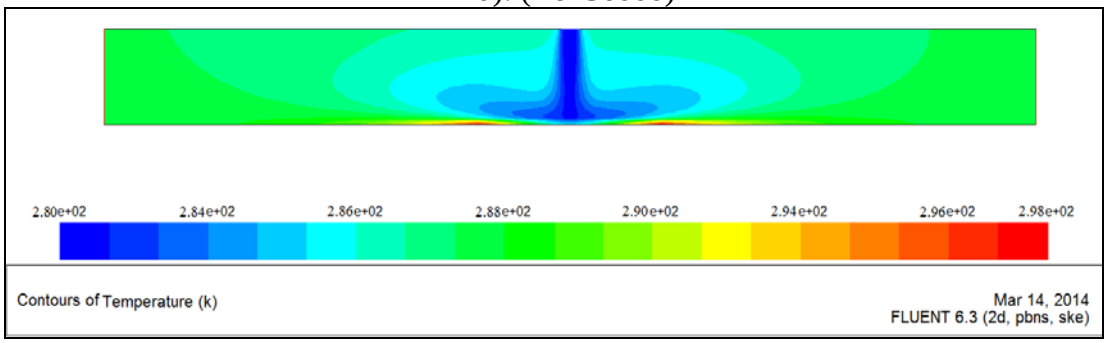

e): (Re=70000)

Fig. (13): Temperature Profile along hot plate surface not covered with metal foam for ($q^{"}$=1500 W/m^2) **(α= 0^o)**

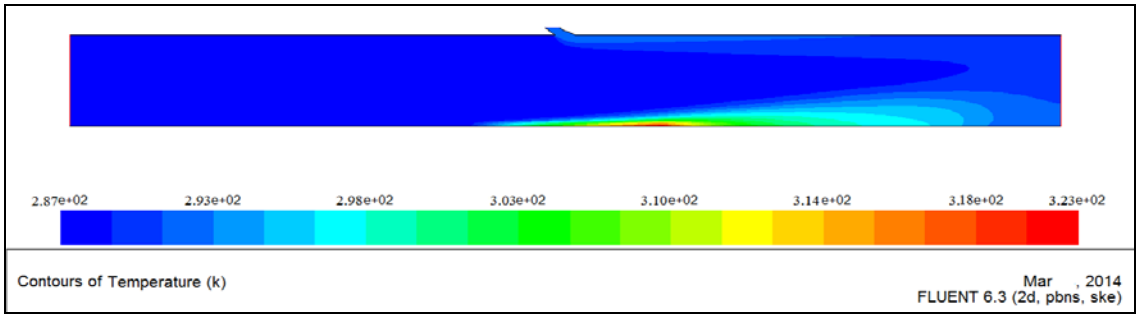

a): (Re=14000)

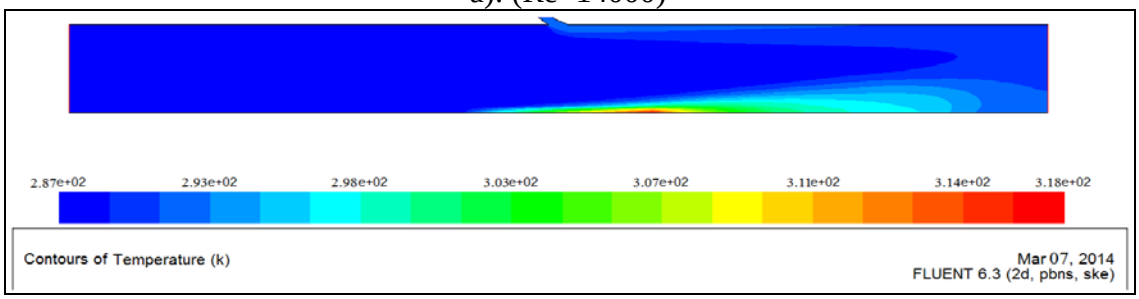

b):
(Re=2800

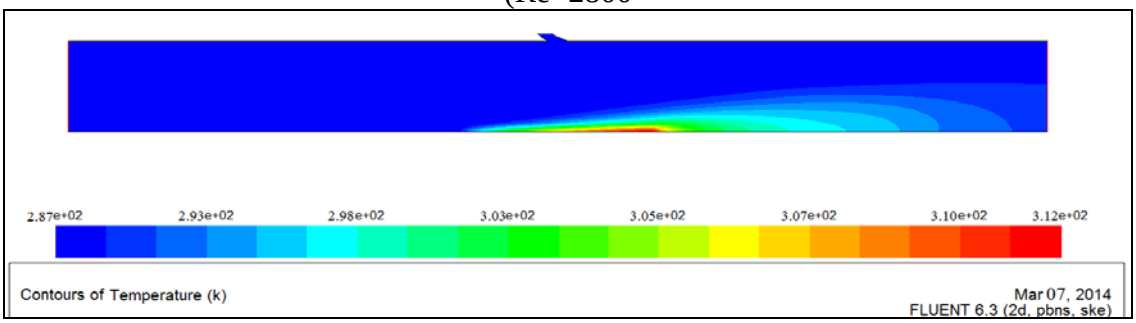

c): (Re=42000)

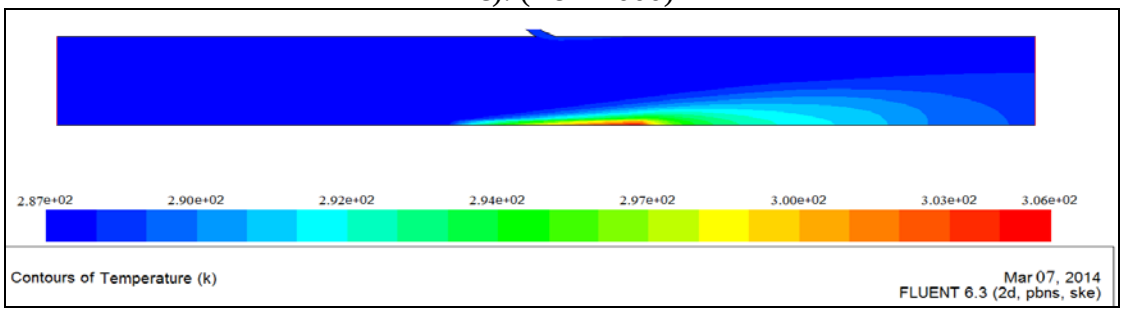

d): (Re=56000)

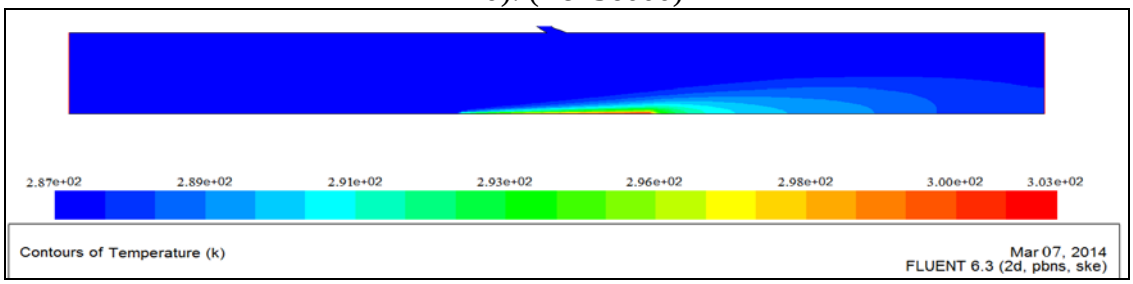

e): (Re=70000)

Fig. (14): Temperature Profile along hot plate surface not covered with metal foam for ($q^{"}$=1500 W/m^2) **(α= 30^o)**

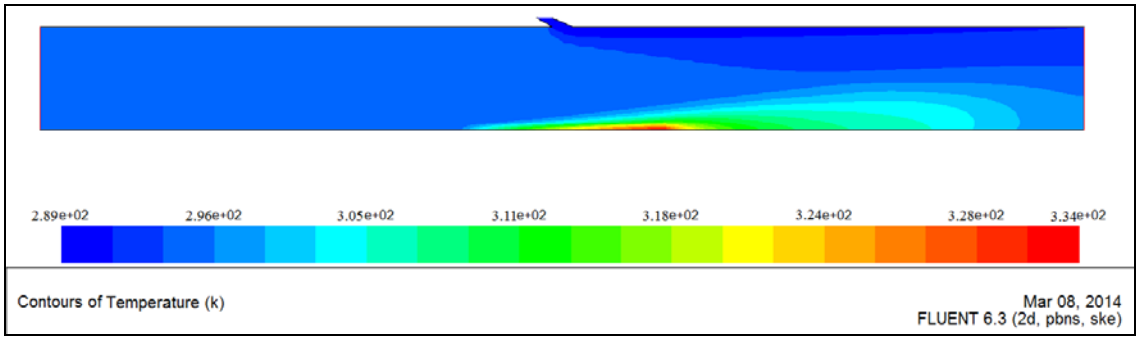

a): (Re=14000)

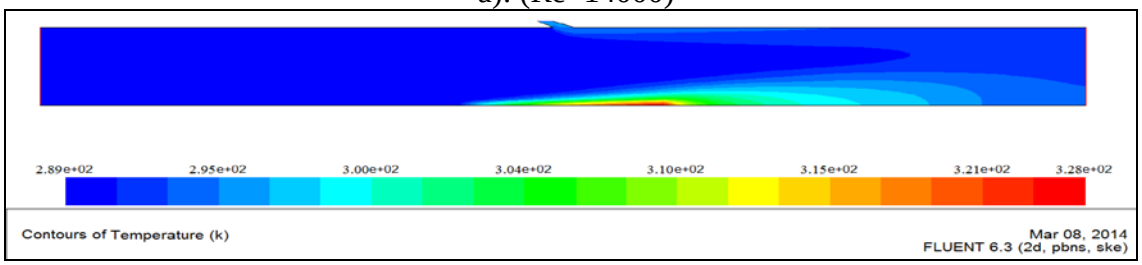

b): (Re=28000)

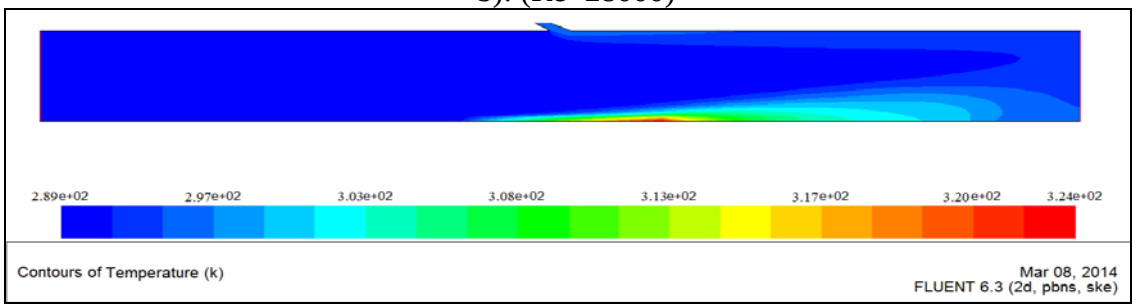

c): (Re=42000)

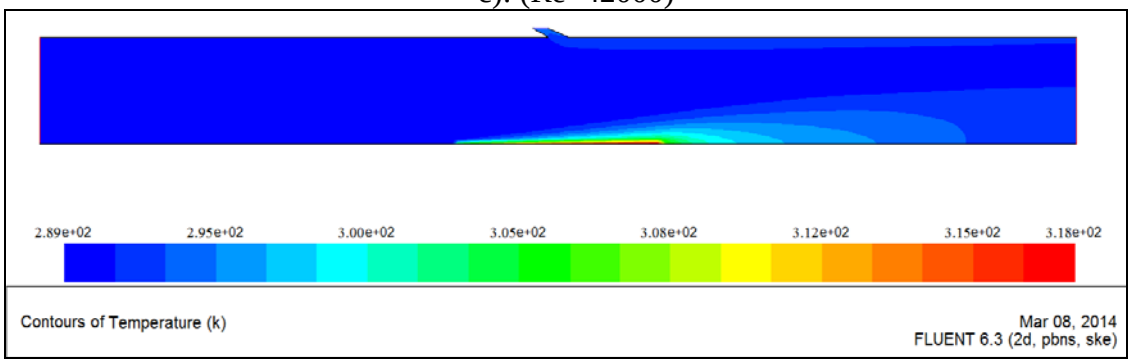

d): (Re=56000)

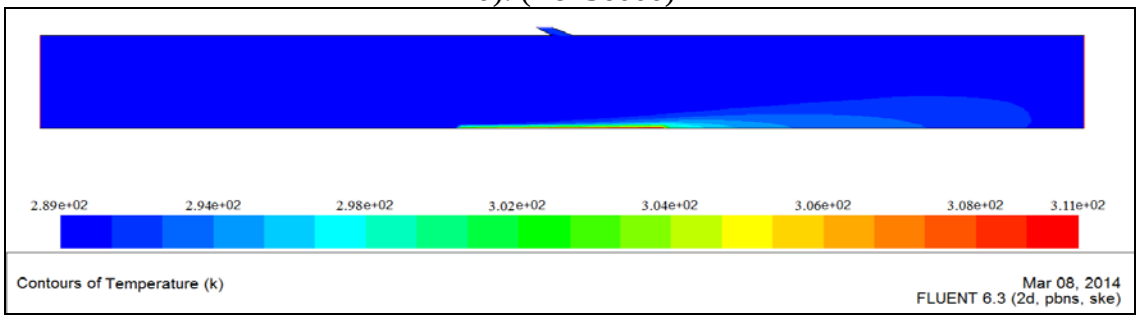

e): (Re=70000)

Fig. (15): Temperature Profile along hot plate surface not covered with metal foam for ($q^{"}$=1500 W/m^2) **(α= 50^o)**

REFERENCES

- Agrawal C., Lyons O.F., Kumar R., Gupta, A. and Murray D., (2013) "Rewetting of a hot horizontal surface through mist jet impingement cooling" International Journal of Heat and Mass Transfer Vol. 58 pp. 188–196.

- Augusto G., Ulson de Souza, Jader R. Barbosa Jr. (2012) "Spray cooling of plain and copper-foam enhanced surfaces". Experimental Thermal and Fluid Science Vol. 39 pp. 198–206.

- Bentarzi F., Mataoui A. and Rebay M. (2011) "Unsteady Simulation Of In Two Turbulent Plane Jets Impinging a Hot Wall" Fifth International Conference on Advanced Computational Methods in Engineering.

- Bastawros A. F., (1998) "Effectiveness of Open-Cell Metallic Foams for High Power Electronic Cooling", Proceeding Symposium on the Thermal Management of Electronics, IMECE. Anaheim, CA.

- Chen a C.C., Huang P.C. and Hwang H.Y ., (2013) "Enhanced forced convective cooling of heat sources by metal-foam porous layers". International Journal of Heat and Mass Transfer Vol. 58 pp. 356–373.
- Colucci.W and Viskanta.R (1996) "Effect of Nozzle Geometry on Local Convective Heat Transfer to a Confined Impinging Air Jet", Experimental Thermal and Fluid Science; 13:71-80 D.

- Crafton J. W.(2004) " The Impingement of Sonic and Sub-Sonic Jets on to a Flat Plate at Inclined Angles ". PhD. thesis, University of Purdue.

- Fluent version 6.2.16 user manual.

- Holman J.P. (1989):"experimental methods for engineers" 5th ed. McGraw-Hill College; 1988.

- Jang S. P., Kim S. J. and Paik K. W. (2003) "Experimental Investigation of Thermal Characteristics For a Microchannel Heat Sink Subject to an Impinging Jet, Using a Micro-thermal Sensor Array" Department of Materials Science and Mechanical Engineering, Korea Advanced Institute of Science and Technology, South Korea,

- Kim, J. and Hyun, J., (2005) "Mixed Convection a Channel With Porous Multi blocks Under Imposed Thermal Modulation", International Journal of Heat and Mass Transfer. Vol. 46, pp. 891-908.

- Kumar R. and Prasad B. V (2011) "Conjugate Heat Transfer From a Flat Plate With Shower Head Impinging Jets", Thermal Turbo machines Laboratory, Department of Mechanical Engineering, Indian Institute of Technology, Madras, Chennai, India,.

- Salas andWaas , (2007) " Convective Heat Transfer in Open Cell Metal Foam" ASME J. Heat Transfer, Vol. 129, pp. 1217-1229.

- Wong., (2012) "Thermal analysis of a metal foam subject to jet impingement" International Communications in Heat and Mass Transfer Vol. 39 pp. 960–965.

- Zhao C.Y., Lu T.J., Hodson H.P. and Jackson, J.D., (2004) "The Temperature Dependence of Effective Thermal Conductivity of Open-Celled Steel Alloy Foams", Vol. 367, pp. 123-131.